JACS
JOURNAL OF THE AMERICAN CHEMICAL SOCIETY

Communication

pubs.acs.org/JACS

Chemical Modification of Graphene via Hyperthermal Molecular Reaction

Girjesh Dubey,*[,†] Roberto Urcuyo,[†] Sabine Abb,[†] Gordon Rinke,[†] Marko Burghard,[†] Stephan Rauschenbach,[†] and Klaus Kern[†,‡]

[†]Max-Planck-Institute for Solid State Research, Heisenbergstrasse 1, 70569 Stuttgart, Germany

[‡]Institut de Physique de la Matière Condensée, École Polytechnique Fédérale de Lausanne, CH-1015 Lausanne, Switzerland

Supporting Information

ABSTRACT: Chemical functionalization of graphene is achieved by hyperthermal reaction with azopyridine molecular ions. The one-step, room temperature process takes place in high vacuum (10^{-7} mbar) using an electrospray ion beam deposition (ES-IBD) setup. For ion surface collisions exceeding a threshold kinetic energy of 165 eV, molecular cation beams of 4,4′-azobis(pyridine) covalently attach to chemical vapor deposited (CVD) graphene. A covalent functionalization degree of 3% of the carbon atoms of graphene is reached after 3−5 h of ion exposure of 2×10^{14} azopyridinium/cm^2 of which 50% bind covalently. This facile approach for the controlled modification of graphene extends the scope of candidate species that would not otherwise react via existing conventional methods.

The emergence of graphene as a 2D Dirac material has ignited a frenzy of study into its distinctive chemical, electronic, magnetic, optical and thermal properties, while broadly uniting scientific efforts across multiple disciplines.[1] Due to the sheer magnitude of mobility exhibited by its ambipolar charge carriers, high speed electronics,[2] integrated circuits,[3] and memories[4] are of particular interest.

Chemical modification of graphene presents a viable pathway for tailoring electronic properties such as band gap[5] and majority carrier type.[6] Covalent functionalization also enables subsequent coupling, which is vital for molecular diagnostics[7] and molecular electronics.[8] Recent strategies include the photochemical decomposition of benzoyl peroxide,[9] azide-modification followed by click-coupling reactions with alkynes,[10] a Diels−Alder reaction of graphene with tetracyanoethylene,[11] and plasma chlorination of graphene.[12] Surface chemists continue to establish reliable protocols to prepare densely ordered, high quality functional monolayers on graphene. The controlled formation of densely ordered and stoichiometric derivatives of graphene remains difficult to attain. Examples of dense terminations include hydrogenation of graphene into fully sp^3-hybridized graphane by exposure to atomic hydrogen[13] and fluorination of graphene into fully sp^3-hybridized fluorographene upon reaction with XeF_2, [14] each of which become wide-gap insulators at complete monolayer coverage.

Hyperthermal ion beams[15,16] of 1−100 eV particle kinetic energy present a unique approach to modification, due to their capability of triggering chemical reactions when their kinetic energy is converted upon collision.[17,18] Molecular ion beams are readily formed by increasingly common methods such as electrospray ionization (ESI).[19]

Here, the covalent modification of graphene via the impact of vibrationally cold, hyperthermal molecular ion collisions is presented. Figure 1a illustrates the gas phase generation of intact, monoprotonated beams of 4,4′-azobis(pyridine) (AZP) from solution using electrospray ionization, which are transferred to vacuum, steered, focused and accelerated toward chemical vapor deposited (CVD) graphene transferred onto SiO_2/n+ Si. The collision energy is adjusted by a Si substrate

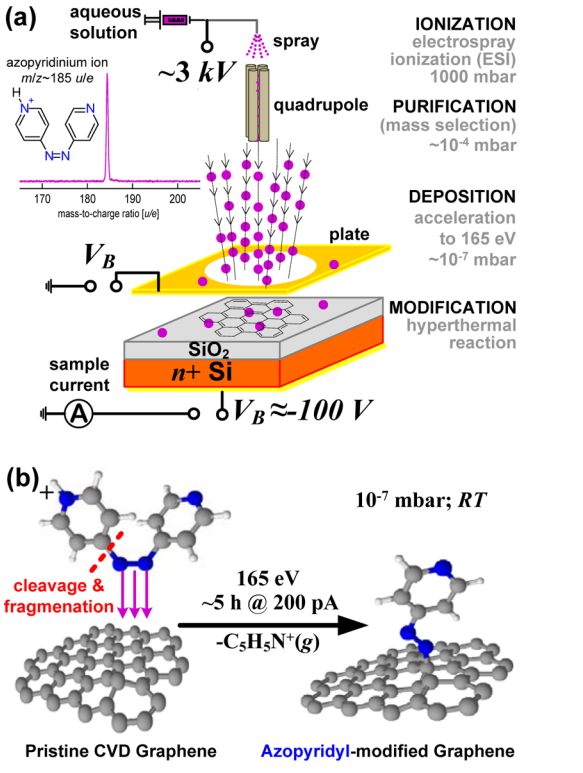

Figure 1. (a) Schematic depiction of the experimental setup for graphene functionalization via hyperthermal reaction. (b) Sketch of the covalent coupling reaction yielding azopyridyl-modified graphene.

Received: May 9, 2014
Published: September 4, 2014

   dx.doi.org/10.1021/ja5046499 | J. Am. Chem. Soc. 2014, 136, 13482−13485

bias V_B. Upon impact, surface induced dissociation cleaves a bond, generating a reactive fragment that covalently bonds to the graphene. Most likely, the cleavage occurs at the C−N bond between the (protonated) pyridine ring and the azo-group, thus generating an azopyridyl-radical as depicted in Figure 1b.

This experiment is made possible by an electrospray ion beam deposition (ES-IBD) system,[20,21] consisting of an ambient nanospray source emitter biased to 3−4 kV, followed by a series of ion optics and differentially pumped stages (see Supporting Information (SI) S-I). Sprays are formed from 1 mM AZP in 1:1 H_2O:EtOH and 0.2% (v/v) formic acid. Time-of-flight mass spectrometry (TOF-MS) (Figure 1a) is used to verify the formation of azopyridinium cations (AZP^+; $m/z \sim 185\ u/e$), and in combination with a mass-selecting quadrupole, a narrow mass-to-charge window is specified so that the reagent is highly purified (>99.99%) before exposure. The beam arrives at the sample through a 4 mm diameter aperture at normal incidence. Corresponding to $V_B = 0$, the primary beam energy (63 ± 3 eV) exiting the quadrupole is first measured by a retarding grid adjacent to the sample. During modification, a deposition current is monitored at the substrate (200−330 pA) and integrated over time such that the coverage is precisely controlled; here the total cation exposure has been set to 1 nA over 1 h, corresponding to a dose of ~2×10^{14} AZP^+/cm^2, which is achieved in 3−5 h, and would correspond to a coverage on the order of a close-packed monolayer assuming a sticking coefficient of unity.

Ex situ ambient confocal Raman scattering (Figure 2a) confirms the characteristic G-Band and 2D-Band of pristine single-layer graphene before deposition.[22] A small D-peak is initially detectable, which has been shown to originate from wrinkles.[23] Upon modification with 165 ± 3 eV ions (V_B = −102 V), a dominant D-peak appears, which is consistent with sp^3-hybridization induced disorder,[24] while suppression of the 2D/G ratio and slight blue-shifted D-peak position further indicates the presence of disorder/doping.[25]

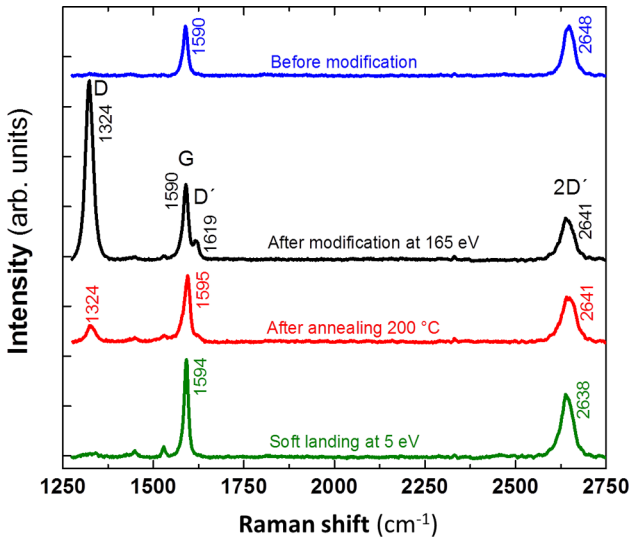

Figure 2. Raman spectra of a CVD graphene sample before and after hyperthermal functionalization with azopyridyl groups, as well as after annealing of the modified sample. Soft landing is shown at the bottom for comparison.

Collisions at 5, 75, 100, and 125 eV produce the same Raman spectrum as that of pristine graphene (Figure 2, lowest spectrum). These depositions can be considered as soft landing. The onset of chemisorption is observed near 165 eV, corresponding to 5.5 eV per covalent bond in the molecule, assuming the center-of-mass translational kinetic energy equipartitions among the internal degrees of freedom in AZP^+, and provided the time-scale of the collision dynamics (~ps) permits particle equalization. An energy density of this order is relatively modest since in actuality it represents the upper limit of a lossless system, yet dissipation into modes of graphene and other nonadiabatic pathways are likely. This activation range is comparable to Landman and co-workers' molecular dynamics calculations of salt cluster collisions on inert surfaces (2.7 eV/particle) leading to fragmentation and dissipation.[26] Empirical data similarly reveals that silver cluster collisions on platinum activate defects/chemisorption above 2.9 eV/Ag.[27] Since single atom vacancies in graphene have been observed[28] after Ar^+ irradiation at considerably high energy densities (140 eV/Ar^+), fragmentation and reactive landing of AZP^+ at 5.5 eV/bond is the most plausible outcome of these collisions.

To confirm the covalent binding of the molecular ions, the modified samples were subjected to thermal treatment. After heating in vacuum at 200 °C for 1 h, Raman spectroscopy revealed a significantly reduced D-peak intensity. This change clearly testifies desorption of chemisorbed molecules.[29] It should be noted that if carbon vacancies created by the ion impact were responsible for the pronounced D-peak, such restoration of the carbon framework of graphene would not be possible, owing to the lack of a suitable carbon source and lack of sufficiently high temperature.[30]

Raman maps displaying the D-peak area over 100 μm^2 regions (SI S-III) show a uniform, large-area modification, which has further been verified over the ~4 mm × 4 mm sample area. At low neutral density filters, the D-peak area is seen to decrease in the direction of the raster scan path, resulting in sloped-maps (SI S-III), which likely arises from desorption due to laser-induced heating.

From the Raman spectra, the average distance L_D [nm], between sp^3-defect centers (i.e., between the covalently attached azopyridyl groups) can be estimated. The intensity ratio of the D and G modes (I_D/I_G) are well above 1 in the spectra of the modified samples, indicative of a high defect density regime, with L_D being on the order of a few nanometers.[31] Upon the basis of the sample-averaged value of $I_D/I_G = 2.5$, the corresponding equation[31] $L_D^2 = 5.4 \times 10^{-2} \cdot E_L^4 \cdot (I_D/I_G)$, where $E_L = 1.96$ eV is the laser excitation energy, yields $L_D \sim 1.4$ nm. This translates into a high functionalization degree of approximately 3%, comparable to the value achievable through extensive hydrogen plasma treatment of graphene.[29] This functionalization degree corresponds to 50% of impacting ions being bound to the graphene. As the elevated collision energy gives rise to competition from elastic scattering,[32] and fragmentation efficiencies close to unity,[33] it is reasonable to attribute the remaining 50% of the collisions to elastic or dissociative projectile scattering and hence no bond formation.

Ambient tapping-mode atomic force microscopy (AFM) shows that despite the modest collision energy supplied to the surface, the pristine topographic quality of CVD graphene is still preserved after exposure, producing highly smooth and flat surfaces. No substantial change in topography or morphology is seen over a 25 μm^2 area. Although an increased roughness is typically reported for graphene modified by the reduction of

dx.doi.org/10.1021/ja5046499 | J. Am. Chem. Soc. 2014, 136, 13482−13485

diazonium salts,[34,35] our AFM observations are consistent with a lower coverage of azopyridyl groups.

The elemental composition and chemical binding at the surface before and after modification was probed by X-ray photoelectron spectroscopy (XPS) using using Al/$K_{\alpha 1}$ photons (1486.7 eV). The C 1s peak of pristine CVD graphene (Figure 3a) has an asymmetric Doniach-Sunjic line-shape, characteristic of sp^2-hybridized C−C.[36]

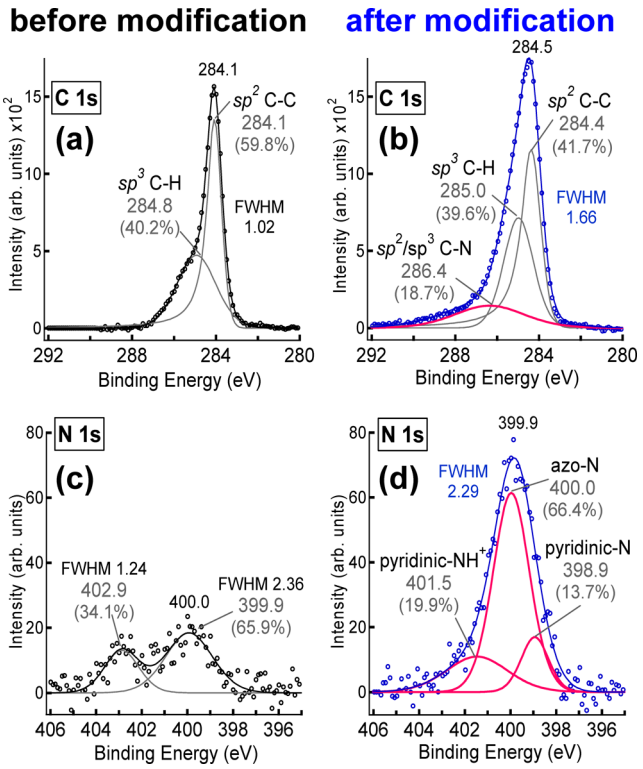

Figure 3. XPS spectra of pristine and hyperthermal-modified graphene (165 eV/cation). (a and b) C 1s; (c and d) N 1s.

Upon modification, the C 1s profile broadens into a three-component envelope (Figure 3b) which can be deconvoluted to reveal the same two peaks matching to the pristine spectrum in Figure 3a, and an additional component centered at 286.4 eV, attributed to sp^2 CN from the pyridyl-terminal group and sp^3 C−N from the azo linkage to graphene.

Upon modification, the C 1s profile broadens into a three-component envelope (Figure 3b), which can be deconvoluted to reveal the same two peaks matching to the pristine spectrum in Figure 3a, and an additional component centered at 286.4 eV, attributed to sp^2 C−N from the pyridyl-terminal group and sp^3 C−N from the azo linkage to graphene.[37]

Compared to the pristine control (Figure 3c), the modified sample shows (Figure 3d) a significantly higher N 1s signal centered at 399.8 eV. The increased N/C ratio is consistent with the deposition of the nitrogen rich AZP or one of its fragments.

The very broad N 1s peak with a full-width at half-maximum of 2.3 eV signifies the presence of multiple types of nitrogen atoms. It can be deconvoluted into pyridine-like nitrogen (389.9 eV), azo-nitrogen (400.0 eV) and protonated pyridine-nitrogen (401.6 eV).[37,38] These binding energies agree with a previous XPS study of 2,2′-azopyridine,[38] reporting a fwhm of 2.7 eV and deconvoluted positions of 389.9 eV for the two nitrogen-pyridinic atoms, and 400.1 eV for the two azo-nitrogens.

For the relative abundance of azo-nitrogen to the combined neutral and protonated pyridinic-nitrogen a ratio of 2:1 is found based on the component areas shown in Figure 3d. This points to a binding mechanism wherein the diimide group cleaves once, preferentially at the protonated pyridyl-site (C_5H_4NH)-N═N-($C_5H_4NH^+$) of the AZP^+ ion beam, producing a neutral azopyridyl-radical (·N═N−C_5H_4N) that binds to graphene through a C−N covalent bond, as illustrated in Figure 1b. The other part, a pyridinium-radical, will rearrange and leave as gaseous protonated pyridine. Protonation of the pyridine groups of 60% detected by XPS thereby likely occurs after exposure to ambient atmosphere rather than originating from the protonated ion beam itself.

Modeling other mechanisms to the nitrogen XPS data resulted in only poor agreement. Should the cleavage have occurred at the nonprotonated pyridyl-site of the AZP^+ ion beam, the resultant azopyridinium-radical and pyridyl-radical could both graft covalently to graphene (yielding a relative abundance of azo to pyridinic nitrogen in the ratio 1:1), or the azopyridinium-radical could rearrange, leaving as gaseous 4-diazenylpyridine, and only the pyridyl-radical would bind (resulting in only pyridinic-nitrogen). However, none of these scenarios are consistent with the intensities of the components in the N 1s peak (Figure 3d). Furthermore, symmetric, azo-initiator-type splitting with nitrogen elimination and concomitant formation of two pyridyl-radicals can also be excluded, as these would not give rise to the azo-nitrogen observed.

Upon the basis of the above observations, covalent linkage of azopyridyl-moieties is the most likely pathway for modification. The hyperthermal activation, however, is a statistical process as well, which can overcome even a high activation barrier. Thus, within the margin of error of the fits, also other less likely reactions may have occurred in parallel.

Hyperthermal ion chemistry presents a unique solution to the challenge of controllably producing dense and ordered monolayers on graphene. Electrospray ionization accommodates both an enormous mass range (1−10^6 Da) and practically unlimited choice of reagents to activate nonequilibrium hyperthermal reactions of graphene that would otherwise remain kinetically unfavorable. High vacuum deposition further minimizes the influence of an electrochemical water/oxygen redox couple at the SiO_2 substrate, which is responsible for doped hysteretic devices in ambient.[39]

The present study demonstrates a one-step nondestructive route to covalently functionalize chemical-vapor-deposited graphene using the controlled deposition of hyperthermal molecular ion beams of azopyridine. Since the kinetic energy of the impinging reagents of 165 eV/ion is significantly larger than that of typical covalent bond-dissociation depths ($1 \leq D_0 \leq 10$ eV/bond), the excess energy supply breaks chemical bonds, and overcomes the costly activation barrier (E_A) that otherwise prohibits addition to the basal plane.[40,41] Raman scattering in combination with XPS demonstrates the formation of a covalently azopyridyl-modified surface with a high functionalization degree of 3%, while AFM imaging shows the resulting graphene retains its topographic integrity.

■ ASSOCIATED CONTENT

Supporting Information

S-I, detailed schematic of the ES-IBD setup; S-II, details on the XPS analysis; S-III, large area modification shown in Raman D

dx.doi.org/10.1021/ja5046499 | J. Am. Chem. Soc. 2014, 136, 13482−13485

band maps. This material is available free of charge via the Internet at http://pubs.acs.org.

AUTHOR INFORMATION

Corresponding Author

Girjesh.Dubey@gmail.com

Notes

The authors declare no competing financial interest.

ACKNOWLEDGMENTS

G.D. acknowledges NSERC (Postdoctoral Fellowship) for support. R.U. acknowledges Universidad de Costa Rica for a doctoral exchange scholarship. We thank Dr. Mitsuharu Konuma for measuring XPS spectra and for useful discussions.

REFERENCES

(1) Geim, A. K.; Novoselov, K. S. *Nat. Mater.* **2007**, *6*, 183.
(2) Lin, Y. M.; Jenkins, K. A.; Valdes-Garcia, A.; Small, J. P.; Farmer, D. B.; Avouris, P. *Nano Lett.* **2009**, *9*, 422.
(3) Lin, Y. M.; Valdes-Garcia, A.; Han, S. H.; Farmer, D. B.; Meric, I.; Dimitrakopoulos, C.; Grill, A.; Avouris, P.; Jenkins, K. A. *Science* **2011**, *332*, 1294.
(4) Stützel, E. U.; Burghard, M.; Kern, K.; Traversi, F.; Nichele, F.; Sordan, R. *Small* **2010**, *6*, 2822.
(5) Bekyarova, E.; Itkis, M. E.; Ramesh, P.; Berger, C.; Sprinkle, M.; de Heer, W. A.; Haddon, R. C. *J. Am. Chem. Soc.* **2009**, *131*, 1336.
(6) Wang, X.; Li, X.; Zhang, L.; Yoon, Y.; Weber, P. K.; Wang, H.; Guo, J.; Dai, H. *Science* **2009**, *324*, 768.
(7) Liu, Y.; Dong, X.; Chen, P. *Chem. Soc. Rev.* **2012**, *41*, 2283.
(8) Sangwan, V. K.; Jariwala, D.; Everaerts, K.; McMorrow, J. J.; He, J.; Grayson, M.; Lauhon, L. J.; Marks, T. J.; Hersam, M. C. *Appl. Phys. Lett.* **2014**, *104*, 083503.
(9) Liu, H.; Ryu, S.; Chen, Z.; Steigerwald, M. L.; Nuckolls, C.; Brus, L. E. *J. Am. Chem. Soc.* **2009**, *131*, 17099.
(10) Devadoss, A.; Chidsey, C. E. D. *J. Am. Chem. Soc.* **2007**, *129*, 5370.
(11) Sarkar, S.; Bekyarova, E.; Niyogi, S.; Haddon, R. C. *J. Am. Chem. Soc.* **2011**, *133*, 3324.
(12) Wu, J.; Xie, L.; Li, Y.; Wang, H.; Ouyang, Y.; Guo, J.; Dai, H. *J. Am. Chem. Soc.* **2011**, *133*, 19668.
(13) Elias, D. C.; Nair, R. R.; Mohiuddin, T. M. G.; Morozov, S. V.; Blake, P.; Halsall, M. P.; Ferrari, A. C.; Boukhvalov, D. W.; Katsnelson, M. I.; Geim, A. K.; Novoselov, K. S. *Science* **2009**, *323*, 610.
(14) Nair, R. R.; Ren, W.; Jalil, R.; Riaz, I.; Kravets, V. G.; Britnell, L.; Blake, P.; Schedin, F.; Mayorov, A. S.; Yuan, S.; Katsnelson, M. I.; Cheng, H.-M.; Strupinski, W.; Bulusheva, L. G.; Okotrub, A. V.; Grigorieva, I. V.; Grigorenko, A. N.; Novoselov, K. S.; Geim, A. K. *Small* **2010**, *6*, 2877.
(15) Grill, V.; Shen, J.; Evans, C.; Cooks, R. G. *Rev. Sci. Instrum.* **2001**, *72*, 3149.
(16) Cyriac, J.; Pradeep, T.; Kang, H.; Souda, R.; Cooks, R. G. *Chem. Rev.* **2012**, *112*, 5356.
(17) Gologon, B.; Green, J. R.; Alvarez, J.; Laskin, J.; Cooks, R. G. *Phys. Chem. Chem. Phys.* **2005**, *7*, 1490.
(18) Volny, M.; Elam, W. T.; Ratner, B. D.; Turecek, F. *Anal. Chem.* **2005**, *77*, 4846.
(19) Fenn, J. B.; Mann, M.; Meng, C. K.; Wong, S. F.; Whitehouse, C. M. *Science* **1989**, *246*, 64.
(20) Rauschenbach, S.; Stadler, F. L.; Lunedei, E.; Malinowski, N.; Koltsov, S.; Costantini, G.; Kern, K. *Small* **2006**, *2*, 540.
(21) Rauschenbach, S.; Vogelgesang, R.; Malinowski, N.; Gerlach, J. W.; Benyoucef, M.; Costantini, G.; Deng, Z.; Thontasen, N.; Kern, K. *ACS Nano* **2009**, *3*, 2901.
(22) Malard, L. M.; Pimenta, M. A.; Dresselhaus, G.; Dresselhaus, M. S. *Phys. Rep.* **2009**, *473*, 51.
(23) Li, X.; Cai, W.; An, J.; Kim, S.; Nah, J.; Yang, D.; Piner, R.; Velamakanni, A.; Jung, I.; Tutuc, E.; Banerjee, S. K.; Colombo, L.; Ruoff, R. S. *Science* **2009**, *324*, 1312.
(24) Koehler, F. M.; Jacobsen, A.; Ihn, T.; Ensslin, K.; Stark, W. J. *Nanoscale* **2012**, *4*, 3781.
(25) Casiraghi, C. *Phys. Status Solidi* **2011**, *248*, 2593.
(26) Cheng, H.; Landman, U. *Science* **1993**, *260*, 1304.
(27) Bromann, K.; Félix, C.; Brune, H.; Harbich, W.; Monot, R.; Buttet, J.; Kern, K. *Science* **1996**, *274*, 956.
(28) Ugeda, M. M.; Brihuega, I.; Guinea, F.; Gómez-Rodríguez, J. M. *Phys. Rev. Lett.* **2010**, *104*, 096804.
(29) Luo, Z.; Yu, T.; Ni, Z.; Lim, S.; Hu, H.; Shang, J.; Liu, L.; Shen, Z.; Lin, J. *J. Phys. Chem. C* **2011**, *115*, 1422.
(30) Daniels, K. M.; Daas, B. K.; Srivastava, N.; Williams, C.; Feenstra, R. M.; Sudarshan, T. S.; Chandrashekhar, M. V. S. *J. Appl. Phys.* **2012**, *111*, 114306.
(31) Ferrari, A. C.; Basko, D. M. *Nat. Nanotechnol.* **2013**, *8*, 235.
(32) Alvarez, J.; Futrell, J. H.; Laskin, J. *J. Phys. Chem. A* **2006**, *110*, 1678.
(33) Dongré, A. R.; Somogyi, A.; Wysocki, V. H. *J. Mass Spectrom.* **1996**, *31*, 339.
(34) Niyogi, S.; Bekyarova, E.; Hong, J.; Khizroev, S.; Berger, C.; de Heer, W.; Haddon, R. C. *J. Phys. Chem. Lett.* **2011**, *2*, 2487.
(35) Sinitskii, A.; Dimiev, A.; Corley, D. A.; Fursina, A. A.; Kosynin, D. V.; Tour, J. M. *ACS Nano* **2010**, *4*, 1949.
(36) Yang, D. Q.; Sacher, E. *Langmuir* **2006**, *22*, 860.
(37) Jansen, R. J. J.; Van Bekkum, H. *Carbon* **1995**, *33*, 1021.
(38) Camalli, M.; Caruso, F.; Mattogno, G.; Rivarola, E. *Inorg. Chimic. Acta.* **1990**, *170*, 225.
(39) Levesque, P. L.; Sabri, S. S.; Aguirre, C. M.; Guillemette, J.; Siaj, M.; Desjardins, P.; Szkopek, T.; Martel, R. *Nano Lett.* **2011**, *11*, 132.
(40) Laskin, J.; Denisov, E.; Futrell, J. *J. Phys. Chem. B* **2001**, *105*, 1895.
(41) Wysocki, V. H.; Kenttämaa, H. I. *J. Am. Chem. Soc.* **1990**, *112*, 5110.